

# The $W^\pm h$ decay channel as a probe of charged Higgs boson production at the Large Hadron Collider

Stefano Moretti<sup>1</sup>

*Rutherford Appleton Laboratory,  
Chilton, Didcot, Oxon OX11 0QX, UK.*

## Abstract

We analyse the chances of detecting charged Higgs bosons of the Minimal Supersymmetric Standard Model (MSSM) at the Large Hadron Collider (LHC) in the  $W^\pm h$  mode, followed by the dominant decay of the lightest Higgs scalar,  $h \rightarrow b\bar{b}$ . If the actual value of  $M_h$  is already known, this channel offers possibly the optimal final state kinematics for charged Higgs discovery, thanks to the narrow resonances appearing around the  $W^\pm$  and  $h$  masses. Besides, within the MSSM, the  $H^\pm \rightarrow W^\pm h$  decay rate is significant for not too large  $\tan \beta$  values, thus offering the possibility of accessing a region of MSSM parameter space left uncovered by other search channels. We consider both strong (QCD) and electroweak (EW) ‘irreducible’ backgrounds in the  $3b$ -tagged channel to the  $gg \rightarrow t\bar{b}H^-$  production process that had not been taken into account in previous analyses. After a series of kinematic cuts, the largest of these processes is  $t\bar{b}W^\pm h$  production in the continuum. However, for optimum  $\tan \beta$ , i.e., between 2 and 3, the charged Higgs boson signal overcomes this background and a narrow discovery region survives around  $M_{H^\pm} \approx 200$  GeV.

---

<sup>1</sup>Electronic mail: moretti@v2.rl.ac.uk

# 1. Introduction

The discovery of charged Higgs bosons [1] will provide a concrete evidence of the multi-doublet structure of the Higgs sector. Recent efforts have focused on their relevance to Supersymmetry (SUSY), in particular in the MSSM, which incorporates exactly two Higgs doublets, yielding – after spontaneous EW symmetry breaking – five physical Higgs states: the neutral pseudoscalar ( $A$ ), the lightest ( $h$ ) and heaviest ( $H$ ) neutral scalars and two charged ones ( $H^\pm$ ).

In much of the parameter space preferred by SUSY, namely  $M_{H^\pm} \geq M_{W^\pm}$  and  $1 < \tan\beta < m_t/m_b$  [2, 3], the LHC will provide the greatest opportunity for the discovery of  $H^\pm$  particles. In fact, over the above  $\tan\beta$  region, the Tevatron (Run 2) discovery potential is limited to charged Higgs masses smaller than  $m_t$  [4].

However, at the LHC, whereas the detection of light charged Higgs bosons (with  $M_{H^\pm} < m_t$ ) is rather straightforward in the decay channel  $t \rightarrow bH^+$  for most  $\tan\beta$  values, thanks to the huge top-antitop production rate, the search is notoriously difficult for heavy masses (when  $M_{H^\pm} > m_t$ ), because of the large reducible and irreducible backgrounds associated with the main decay mode  $H^- \rightarrow b\bar{t}$ , following the dominant production channel  $bg \rightarrow tH^-$  [5]. (Notice that the rate of the latter exceeds by far other possible production modes [6]–[8], this rendering it the only viable channel at the CERN machine in the heavy mass region.)

The analysis of the  $H^- \rightarrow b\bar{t}$  signature has been the subject of many debates [9]–[12], whose conclusion is that the LHC discovery potential is satisfactory, but only provided that  $\tan\beta$  is small ( $\lesssim 1.5$ ) or large ( $\gtrsim 30$ ) enough and the charged Higgs boson mass is below 600 GeV or so.

A recent analysis [13] has shown that the  $\tau\nu$  decay mode, indeed dominant for light charged Higgs states and exploitable below the top threshold for any accessible  $\tan\beta$  [14], can be used at the LHC even in the large  $M_{H^\pm}$  case, in order to discover  $H^\pm$  scalars in the parameter range  $\tan\beta \gtrsim 3$  and  $200 \text{ GeV} < M_{H^\pm} < 1 \text{ TeV}$ . Besides, if the distinctive  $\tau$  polarisation [15] is used in this channel, the latter can provide at least as good a heavy  $H^\pm$  signature as the  $H^- \rightarrow b\bar{t}$  decay mode (for the large  $\tan\beta$  regime [16, 17]).

At present then, it is the  $\tan\beta \lesssim 3$  region of the MSSM which ought to be explored through other decay modes, especially those where direct mass reconstruction is possible. The most obvious of these is the  $H^\pm \rightarrow W^{\pm(*)}h$  channel [18] (see also [19]), proceeding via the production of a charged gauge boson and the lightest Higgs scalar of the MSSM, with the former on- or off-shell depending on the relative values of  $M_{H^\pm}$  and  $M_h$ . In fact, its branching ratio (BR) can be rather large, competing with the bottom-top decay mode and overwhelming the tau-neutrino one for  $M_{H^\pm} \gtrsim m_t$  at low  $\tan\beta$ : see Figs. 1–2. Besides, under the assumption that the  $h$  scalar has previously been discovered (which we embrace here), its kinematics is rather constrained, around two resonant decay modes,  $W^\pm \rightarrow 2 \text{ jets}$  (or lepton-neutrino) and  $h \rightarrow b\bar{b}$ , an aspect which allows for a significant reduction of the QCD background. As demonstrated in Ref. [20], signals of charged Higgs bosons in the  $2 \lesssim \tan\beta \lesssim 3$  range can be seen in this channel, provided that  $200 \text{ GeV} \lesssim M_{H^\pm} \lesssim 220 \text{ GeV}$  (see also [21] for an experimental simulation). The above lower limit on  $\tan\beta$  corresponds to the border of the exclusion region drawn from LEP2 direct searches for the MSSM  $h$  scalar, whose mass bound is

now set at  $M_h \gtrsim 100$  GeV or so [22].

It is the purpose of this letter that of resuming the studies of Ref. [20], by analysing the contribution to the background due to several irreducible processes, not considered there, whose presence could spoil the feasibility of charged Higgs searches in the  $W^{\pm(*)}h$  mode of the MSSM.

The plan of this paper is as follows. In the next Section we discuss possible signals and backgrounds, their implementation and list the values adopted for the various parameters needed for their computation. Section 3 is devoted to the presentation and discussion of the results. Conclusions are in Section 4.

## 2. Signals and backgrounds

We generate the signal cross sections by using the formulae of Ref. [11]. That is, we implement the  $2 \rightarrow 3$  matrix element (ME) for the process

$$gg \rightarrow t\bar{t}H^- + \text{charge conjugate (c.c.)}. \quad (1)$$

This nicely embeds both the  $gg \rightarrow t\bar{t} \rightarrow t\bar{t}H^- + \text{c.c.}$  subprocess of top-antitop production and decay, which is dominant for  $m_t \gtrsim M_{H^\pm}$ , as well as the  $bg \rightarrow tH^- + \text{c.c.}$  one of  $b\bar{t}$ -fusion and  $H^\pm$ -bremsstrahlung, which is responsible for charged Higgs production in the case  $m_t \lesssim M_{H^\pm}$  [23]. The ME of process (1) has been computed by means of the spinor techniques of Refs. [24]–[27].

In the  $H^- \rightarrow W^{-(*)}h \rightarrow W^{-(*)}b\bar{b}$  channel, assuming high efficiency and purity in selecting/rejecting  $b$ -/ $\text{non-}b$ -jets, possible irreducible background processes are the following (we consider only the  $gg$ -initiated channels):

1. the  $t\bar{t}W^-h$  continuum;
2.  $t\bar{t}W^-Z$  production, especially when  $M_Z \approx M_h$ ;
3. the QCD induced case  $t\bar{t}W^-g$ ;
4. and, finally,  $t\bar{t}W^-H$  and  $t\bar{t}W^-A$  intermediate states;

in which  $H, h, A, Z, g \rightarrow b\bar{b}$ , plus their c.c. channels. Once the top quark appearing in the above reactions decays, two  $W^\pm$  bosons are present in each event. We will eventually assume the  $W^+W^-$  pair to decay semi-leptonically to light-quark jets, electrons/muons and corresponding neutrinos. Furthermore, we will require to tag exactly three  $b$ -jets in the final state (e.g., by using  $\mu$ -vertex or high  $p_T$  lepton techniques). The same ‘signature’ was considered in Ref. [20], where only the ‘intrinsic’  $t\bar{t}H^- \rightarrow t\bar{t}b\bar{b}$  background and the QCD noise due to ‘ $t\bar{t} + \text{jet}$ ’ events were studied (with jet signifying here either a  $b$ -, light-quark or gluon jet, the latter two mistagged for the former).

Both signal and background MEs have been integrated numerically by means of VEGAS [28] and, for test purposes, of RAMBO [29] and Metropolis [30] as well. While proceeding to the phase space integration, one also has to fold in the  $(x, Q^2)$ -dependent Parton Distribution Functions (PDFs) for the two incoming gluons. These have been evaluated at leading-order, by means of the package MRS-LO(05A) [31].

The numerical values of the SM parameters are ( $\ell = e, \mu$ ):

$$\begin{aligned}
m_\ell &= m_{\nu_\ell} = m_u = m_d = m_s = m_c = 0, \\
m_b &= 4.25 \text{ GeV}, \quad m_t = 175 \text{ GeV}, \\
M_Z &= 91.2 \text{ GeV}, \quad \Gamma_Z = 2.5 \text{ GeV}, \\
M_{W^\pm} &= 80.2 \text{ GeV}, \quad \Gamma_W = 2.2 \text{ GeV}.
\end{aligned} \tag{2}$$

As for the top width  $\Gamma_t$ , we have used the LO value calculated within the MSSM (i.e.,  $\Gamma_t = 1.55 \text{ GeV}$  if  $M_{H^\pm} \gg m_t$ ).

Concerning the MSSM parameters, we proceed as follows. For a start, we assume that the mass of the lightest neutral Higgs particle (but not  $\tan\beta$ ) is already known, thanks to its discovery at either LEP2, Tevatron (Run 2) or from early analyses at the LHC itself. Thus, for us,  $M_h$  is a fixed parameter, assuming for reference the following discrete values: e.g., 90, 100, 110, 120 and 130 GeV. Then we express all other Higgs masses as a function of  $M_{H^\pm}$  and  $\tan\beta$ . For the pseudoscalar Higgs boson mass, the tree-level relation  $M_{H^\pm}^2 = M_{W^\pm}^2 + M_A^2$  is assumed. Radiative corrections then, of arbitrary perturbative order, are in practice embedded in the  $H$  mass and the mixing angle  $\alpha$ . In general, notice that, at the ‘Renormalisation Group improved’ one-loop level [32], it is only for very large values of the lightest stop mass and of the squark mixing parameters that  $M_h$  can escape the LEP2 bound in the low  $\tan\beta$  region, on which we will focus most of our attention.

Finally, notice that we develop our discussion at the parton level, without considering fragmentation and hadronisation effects. Thus, jets are identified with the partons from which they originate and all cuts are applied directly to the latter. In particular, when selecting  $b$ -jets, a vertex tagging is implied, with a finite efficiency,  $\epsilon_b$ , per each tag. Moreover, we assume no correlations among multiple tags, nor do we include misidentification of light-quark (including  $c$ -quark-)jets produced in  $W^\pm$  decays as  $b$ -jets.

### 3. Results and discussion

As a preliminary exercise, we study the total production and decay cross sections before any cuts, as all our reactions are finite over their entire phase spaces (recall that  $m_b \neq 0$ ). This is done in Figs. 3–4 for the signal and the five background processes discussed in the previous Section, for five values of  $\tan\beta$ , over the range  $140 \text{ GeV} \lesssim M_{H^\pm} \lesssim 500 \text{ GeV}$ , for  $M_h = 90$  and  $100 \text{ GeV}$ , in the channel  $X \rightarrow b\bar{b}$ , where  $X = h, Z, g, H$  or  $A$ . (Of course, the  $W^\pm Z$  and  $W^\pm g$  backgrounds have no dependence on any of the three parameters above<sup>2</sup>.) As for the decay rates of the top (anti)quark and the  $W^\pm$  boson, for sake of simplicity, we take them equal to 1 for the time being. The signal is always dominated by the QCD background and – at large  $\tan\beta$  – also by the EW ones. Notice the local maxima of the signal rates at  $M_{H^\pm} \approx M_{W^\pm} + M_h$ , as induced by the opening of the  $H^- \rightarrow W^- h$  decay (compare to Figs. 1–2), and the minima as well, due to the onset of the  $H^- \rightarrow b\bar{t}$  channel instead.

---

<sup>2</sup>Note that the rates in Figs. 3–4 account for the c.c. production modes as well.

In the reminder of our analysis, we assume semi-leptonic decays of  $W^+W^-$  pairs, as in Ref. [20]: i.e.,  $W^+W^- \rightarrow 2 \text{ jets } \ell^\pm \nu_\ell$  (hereafter, jet refers to a non- $b$ -jet and  $\ell = e, \mu$ ). However, as compared to that analysis, we make one simplification. Namely, we assume that *one* top (anti)quark and the  $W^\pm$  boson generated in its decay have already been reconstructed, e.g., by using the mass selection procedure advocated in Ref. [20], either leptonically or hadronically. This allows us to greatly reduce the complexity of our numerical calculation while – we believe – substantially un-affecting the relative rates of signal and backgrounds (in fact, all processes described produce the same final state and all involve at least one top quark). Then we apply the following cuts on the remaining particles (here, the label  $j$  refers to the decay products of the second  $W^\pm$  boson present in the event, which can be either light-quarks or leptons):

$$p_T(b, j, \text{missing}) > 20 \text{ GeV} \quad (3)$$

on the transverse momentum (including the missing one),

$$|\eta(b, j)| < 2.5 \quad (4)$$

on the pseudorapidity, and

$$\Delta R(bb, bj, jj) > 0.4 \quad (5)$$

on the relative separation of  $b$ - and light-quark jets/leptons  $j$ , where

$$\Delta R(ij) = \sqrt{\Delta\eta(ij)^2 + \Delta\phi(ij)^2}, \quad (6)$$

is defined in terms of relative differences in pseudorapidity  $\eta(ij)$  and azimuth  $\phi(ij)$ , with  $i \neq j = b, j/\ell$ . Furthermore, we impose (see also Ref. [20])

$$|M_{bb} - M_h| < 10 \text{ GeV} \quad (7)$$

on exactly one pair of  $b$ -jets,

$$M_{jj} > 50 \text{ GeV} \quad (8)$$

on the light-jet (or lepton-neutrino) pair (recall that the  $W^\pm$  can be off-shell), and, finally,

$$|M_{bbbjj} - M_t| < 20 \text{ GeV} \quad (9)$$

around the top mass if three  $b$ 's are present in the event (in addition to the one already used to reconstruct the top (anti)quark). In such a case, one may assume that the charged Higgs boson has predominantly been produced in the decay of a top (anti)quark (when  $M_{H^\pm} \lesssim m_t$ ). If instead only two appear, then one should conclude that the Higgs has mainly been generated in a bremsstrahlung/fusion process (because  $M_{H^\pm} \gtrsim m_t$ ) with a  $b$ -(anti)quark lost along the beam pipe. Our  $2 \rightarrow 3$  production mechanism naturally allows one to emulate both dynamics in a gauge invariant fashion, including all interference effects. As already mentioned, however, we will assume a triple  $b$ -tagging, this implying an overall efficiency factor of  $\epsilon_b^3$  multiplying our signal and background rates. (Thus, the third  $b$ -jet in eq. (9) is actually non- $b$ -tagged: it can be interpreted as the jet system satisfying neither eq. (7) nor eq.(8).) We take  $\epsilon_b = 0.5$ , like in [20, 21] (and assume 100% lepton identification efficiency).

Given the signal production rates before acceptance and selection cuts, it is clear that – for such an  $\epsilon_b$  – even at high collider luminosity (i.e.,  $\int \mathcal{L} dt = 100 \text{ fb}^{-1}$  per annum), hopes of disentangling the charged Higgs boson of the MSSM in the  $W^{\pm(*)}h$  decay channel are only confined to the very low  $\tan\beta$  region. We will thus restrict ourselves to study in the reminder of the paper  $\tan\beta$  values which are, e.g., below seven. The total signal rates after the cuts (3)–(9) have been applied can be found in Fig. 5, for the choices  $\tan\beta = 1, 2, 3$  and 7, as a function of  $M_{H^\pm}$ . For reference, we illustrate the ‘borderline’ case  $M_h = 100 \text{ GeV}$ . (Indeed, a lower  $M_h$  value at  $\tan\beta = 2$  is in contradiction with LEP2 data, whereas higher masses induce a far too large suppression on  $\text{BR}(H^\pm \rightarrow W^{\pm(*)}h)$ : see Fig. 2.) The trends in the figure are the consequence of two effects. On the one hand, the production cross section of  $gg \rightarrow t\bar{b}H^- + \text{c.c.}$  is roughly proportional to  $(m_t^2 \cot^2\beta + m_b^2 \tan^2\beta)$ , so that its maxima occur at very low or very high  $\tan\beta$ . On the other hand, we have seen how the largest  $H^- \rightarrow W^{-(*)}h$  decay fraction is attained for  $\tan\beta \approx 2$ . In the end, the largest values for  $\sigma(gg \rightarrow t\bar{b}H^-) \times \text{BR}(H^- \rightarrow W^{-(*)}h) + \text{c.c.}$  are obtained for  $\tan\beta = 1$ : see Fig. 5. Unfortunately, such a  $\tan\beta$  value is already excluded in the MSSM from LEP2 data [20]. For the optimal remaining choice, i.e.,  $\tan\beta = 2$ , the annual rate never exceeds 140 events (before any  $b$ -tagging efficiency but after acceptance and selection cuts). The maximum occurs at  $M_{H^\pm} \approx 200 \text{ GeV}$ , significantly above the real threshold at  $M_h + M_{W^\pm} \approx 180 \text{ GeV}$ .

We now compare such a signal with the irreducible backgrounds 1.–4., for the same choice of  $\tan\beta$  and  $M_h$  (where relevant). This is done in the upper half of Fig. 6, at the level of total production rates. After the cuts (3)–(9) are enforced, all background components in 2.–4. are overwhelmed by the signal in the vicinity of  $M_{H^\pm} = 200 \text{ GeV}$ , whereas the  $W^\pm h$  continuum production is always larger than the  $H^\pm \rightarrow W^\pm h$  resonant channel. Thus, it is relevant to compare the last two processes in the ‘reconstructed’ invariant mass  $M_{W^\pm h}$ , i.e., that obtained from pairing the two  $b$ -jets fulfilling condition (7) and the two light-quark jets (or, alternatively, the lepton-neutrino pair) satisfying eq. (8) and not already reconstructing  $M_{W^\pm}$  on their own and  $m_t$  in association with any of the  $b$ ’s (see Ref. [20]). The spectrum in this variable is presented in the lower half of Fig. 6, for our ideal case  $M_{H^\pm} = 200 \text{ GeV}$  (and, again,  $\tan\beta = 2$  and  $M_h = 100 \text{ GeV}$ ). For such MSSM parameter combination, the charged Higgs signal is well above the continuum for values of  $M_{W^\pm h}$  which are  $\pm 20 \text{ GeV}$  from  $M_{H^\pm}$ . (To vary  $M_{H^\pm}$  and/or  $\tan\beta$  basically corresponds to rescale the solid line in the last plot by a constant factor, according to the rates in Fig. 5.)

For reference, Tab. 1 presents the number of events of resonant and continuum  $W^\pm h$  production at the LHC, after 300 inverse femtobarns of collected luminosity, for  $\epsilon_b^3 = 0.125$ , in the window  $|M_{H^\pm} - M_{W^\pm h}| < 40 \text{ GeV}$ , for the three values  $M_{H^\pm} = 180, 200$  and  $220 \text{ GeV}$ . Although very small, a  $H^- \rightarrow W^- h$  signal is generally observable above the  $W^- h$  continuum for  $M_{H^\pm}$  around  $200 \text{ GeV}$ . Our numbers are roughly consistent with those in Ref. [20], if one considers that we neglect the finite efficiency of reconstructing one  $W^\pm$  boson and the associated top (anti)quark and since we have chosen somewhat different cuts. Therefore, in the end, the dominant backgrounds remain (in the  $3b$ -tagged channel) the  $H^- b\bar{t} + \text{c.c.}$  decay and the QCD noise involving misidentified gluons, i.e., those already identified in Ref. [20].

## 4. Conclusions

In summary, in this paper, we have complemented a previous analysis [20] of the production and decay of charged Higgs bosons of the MSSM at the LHC, in the channels  $gg \rightarrow t\bar{b}H^-$  and  $H^- \rightarrow W^{-(*)}h$  (and charged conjugated modes), respectively, by considering several irreducible backgrounds in the  $3b$ -tagged channel, i.e.,  $t\bar{b}H^- + \text{c.c.} \rightarrow 3b \text{ 2 jets } \ell + \text{‘missing energy’}$  (where the initial  $b$ -(anti)quark is usually lost along the beam pipe), which had not yet been considered.

We have found that, after standard acceptance cuts and a kinematic selection along the lines of the one outlined in Ref. [20], the dominant background among those considered here is the continuum production  $gg \rightarrow t\bar{b}W^{-(*)}h + \text{c.c.}$  However, the latter has been found to lie significantly below the signal in the only region where this is detectable: when  $\tan\beta \approx 2 - 3$  and  $M_{H^\pm} \approx 200$  GeV (with  $M_h$  around 100 GeV, close to the latest LEP2 constraints). Thus, the chances of detecting the  $H^- \rightarrow W^-h \rightarrow W^-b\bar{b}$  decay in such a (narrow) region of the MSSM parameter space depend mainly on the interplay between this mode, the competing one  $H^- \rightarrow b\bar{t} \rightarrow W^-b\bar{b}$  and the QCD background with mistagged gluons, as are the latter two that clearly overwhelm the former (recall the last figure in [20]).

We have carried out our analysis at parton level, without showering and hadronisation effects but emulating typical detector smearing. We are confident that its salient features should survive a more sophisticated simulation, such as the one presented in Ref. [21]. Besides, our results concerning the backgrounds can be transposed to the case of non-minimal SUSY models (where the  $H^\pm$  discovery potential can extend to a much larger portion of parameter space), such as those considered in Ref. [20], so that also in these scenarios the irreducible backgrounds analysed here can be brought under control.

## Acknowledgements

The author is grateful to the UK-PPARC for financial support. Furthermore, he thanks D.P. Roy for his remarks, which induced him to eventually considering the subject of this research. He also thanks K.A. Assamagan for several useful discussions. Finally, many conversations with K. Odagiri are acknowledged, as well as many numerical comparisons against and the use of some of his programs.

## References

- [1] J.F. Gunion, H.E. Haber, G.L. Kane and S. Dawson, “The Higgs Hunter Guide” (Addison-Wesley, Reading MA, 1990).
- [2] CMS Technical Proposal, CERN/LHC/94-43 LHCC/P1, December 1994.
- [3] ATLAS Technical Proposal, CERN/LHC/94-43 LHCC/P2, December 1994.
- [4] CDF Collaboration, *Phys. Rev. Lett.* **79** (1997) 357; D0 Collaboration, *Phys. Rev. Lett.* **82** (1999) 4975.

- [5] J.F. Gunion, H.E. Haber, F.E. Paige, W.-K. Tung and S.S.D. Willenbrock, *Nucl. Phys.* **B294** (1987) 621.
- [6] S. Moretti and K. Odagiri, *Phys. Rev.* **D55** (1997) 5627.
- [7] A.A. Barrientos Bendeuzú and B.A. Kniehl, *Phys. Rev.* **D59** (1999) 015009.
- [8] S. Moretti and K. Odagiri, *Phys. Rev.* **D59** (1999) 055008.
- [9] V. Barger, R.J.N. Phillips and D.P. Roy, *Phys. Lett.* **B324** (1994) 236.
- [10] J.F. Gunion and S. Geer, preprint UCD-93-32, September 1993, [hep-ph/9310333](#); J.F. Gunion, *Phys. Lett.* **B322** (1994) 125.
- [11] D.J. Miller, S. Moretti, D.P. Roy and W.J. Stirling, *Phys. Rev.* **D61** (2000) 055011.
- [12] S. Moretti and D.P. Roy, *Phys. Lett.* **B470** (1999) 209.
- [13] K. Odagiri, preprint RAL-TR-1999-012, February 1999, [hep-ph/9901432](#).
- [14] S. Raychaudhuri and D.P. Roy, *Phys. Rev.* **D53** (1996) 4902.
- [15] B.K. Bullock, K. Hagiwara and A.D. Martin, *Phys. Rev. Lett.* **67** (1991) 3055; *Nucl. Phys.* **B395** (1993) 499.
- [16] D.P. Roy *Phys. Lett.* **B459** (1999) 607.
- [17] K.A. Assamagan, ATLAS Internal Note ATL-PHYS-99-013 (1999); K.A. Assamagan, A. Djouadi, M. Drees, M. Guchait, R. Kinnunen, J.L. Kneur, D.J. Miller, S. Moretti, K. Odagiri and D.P. Roy, contribution to the Workshop ‘Physics at TeV Colliders’, Les Houches, France, 8-18 June 1999, [hep-ph/0002258](#) (to appear in the proceedings).
- [18] S. Moretti and W.J. Stirling, *Phys. Lett.* **B347** (1995) 291; Erratum, *ibidem* **B366** (1996) 451.
- [19] E. Barradas, J.L. Diaz-Cruz, A. Gutierrez and A. Rosado, *Phys. Rev.* **D53** (1996) 1678; A. Djouadi, J. Kalinowski and P.M. Zerwas, *Z. Phys.* **C70** (1996) 435; E. Ma, D.P. Roy and J. Wudka, *Phys. Rev. Lett.* **80** (1998) 1162.
- [20] M. Drees, M. Guchait and D.P. Roy, *Phys. Lett.* **B471** (1999) 39.
- [21] K.A. Assamagan, ATLAS Communication ATL-PHYS-99-025 (1999); K.A. Assamagan, A. Djouadi, M. Drees, M. Guchait, R. Kinnunen, J.L. Kneur, D.J. Miller, S. Moretti, K. Odagiri and D.P. Roy, in Ref. [17].
- [22] See, e.g.: LEP Higgs Working Group, <http://www.cern.ch/LEPHIGGS/>.
- [23] J.L. Diaz-Cruz and O.A. Sampayo, *Phys. Rev.* **D50** (1994) 6820; F. Borzumati, J.L. Kneur and N. Polonsky, *Phys. Rev.* **D60** (1999) 115011.
- [24] R. Kleiss and W.J. Stirling, *Nucl. Phys.* **B262** (1985) 235.



- [25] F.A. Berends, P.H. Daverveldt and R. Kleiss, *Nucl. Phys.* **B253** (1985) 441.
- [26] C. Mana and M. Martinez, *Nucl. Phys.* **B287** (1987) 601.
- [27] S. Moretti, *Phys. Rev.* **D50** (1994) 2016.
- [28] G.P. Lepage, *Jour. Comp. Phys.* **27** (1978) 192.
- [29] R. Kleiss, W.J. Stirling and S.D. Ellis, *Comput. Phys. Commun.* **40** (1986) 359.
- [30] H. Kharraziha and S. Moretti, preprint DESY 99-133, RAL-TR-1999-061, TSL/ISV-99-0216, September 1999, [hep-ph/9909313](#).
- [31] A.D. Martin, R.G. Roberts, W.J. Stirling and R.S. Thorne, *Phys. Lett.* **B443** (1998) 301.
- [32] H.E. Haber, R. Hempfling and A.H. Hoang, *Z. Phys.* **C75** (1997) 539; M. Carena, J. Espinosa, M. Quiros and C. Wagner, *Phys. Lett.* **B355** (1995) 209.

Number of events after 300 fb <sup>-1</sup> (including c.c. channels)			
tan $\beta = 2$		$M_h = 100$ GeV	
$M_{H^\pm}$ (GeV)	$t\bar{b}H^-$	$t\bar{b}W^-h$	$S/\sqrt{B}$
180	34	6	13
200	52	11	16
220	27	17	7
MRS-LO(05A)			
$3b$ -tag		All cuts	

Table 1: Number of signal ( $S$ ,  $t\bar{b}H^-$ ) and dominant background ( $B$ ,  $t\bar{b}W^-h$ ) events, along with the statistical significance  $S/\sqrt{B}$ , after the implementation of the cuts (3)–(9) in the decay channel  $W^+W^-h \rightarrow 2 \text{ jets } \ell^\pm \nu_\ell b\bar{b}$ . Rates are given for  $\tan \beta = 2$ ,  $M_h = 100$  GeV, three choices of  $M_{H^\pm}$ , as obtained by using the MRS-LO(05A) set of PDFs, after 300 fb<sup>-1</sup> of luminosity and for  $\epsilon_b = 0.5$ .

### Charged Higgs Branching Ratios

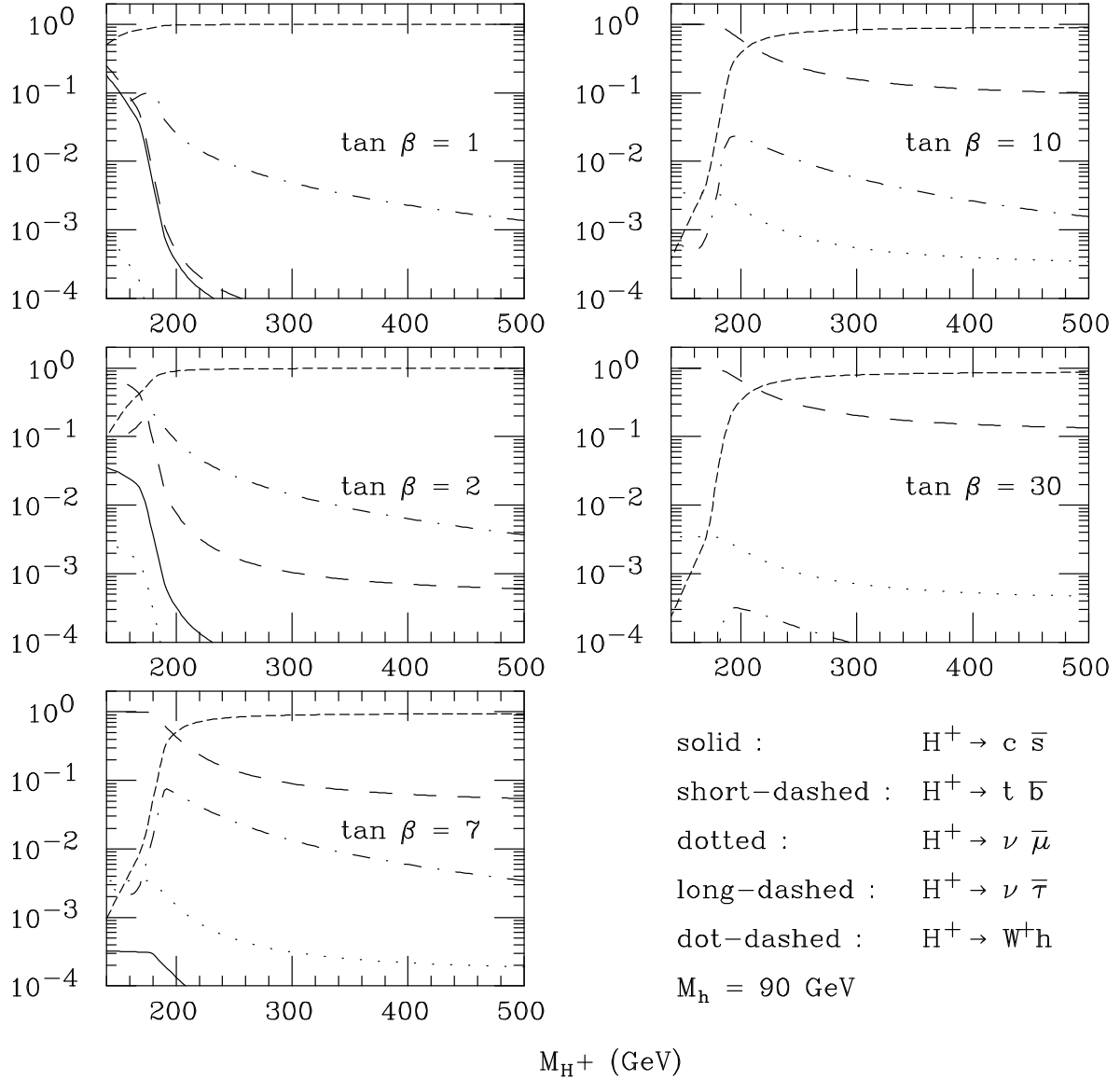


Figure 1: Dominant branching ratios of the charged Higgs boson of the MSSM for selected values of  $\tan \beta$  over the mass range  $140 \text{ GeV} \lesssim M_{H^\pm} \lesssim 500 \text{ GeV}$ . The mass of the lightest Higgs boson has been fixed at  $M_h = 90 \text{ GeV}$ .

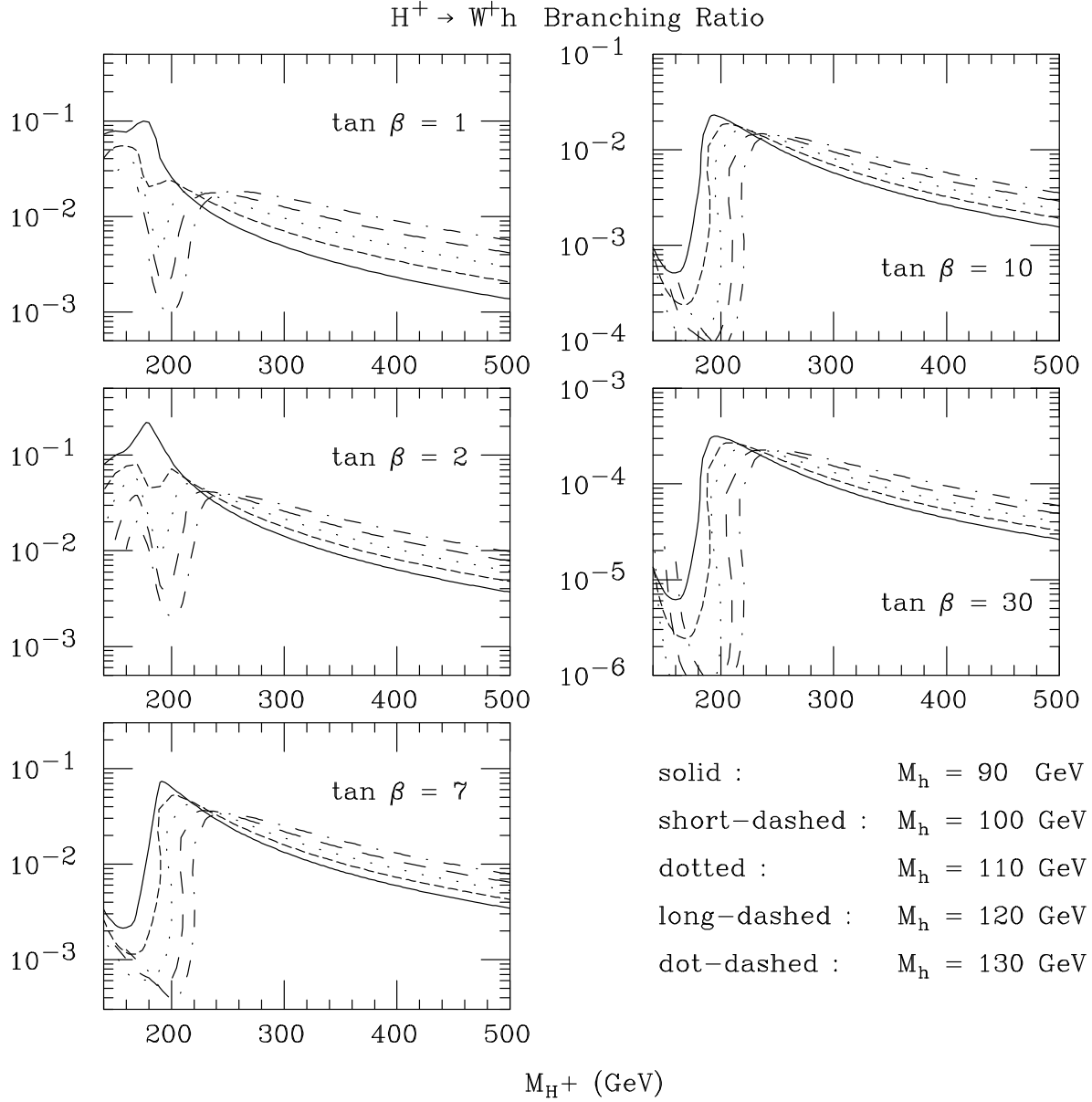


Figure 2: Branching ratios into  $W^\pm h$  pairs of the charged Higgs boson of the MSSM for selected values of  $\tan \beta$  over the mass range  $140 \text{ GeV} \lesssim M_{H^\pm} \lesssim 500 \text{ GeV}$ . The mass of the lightest Higgs boson has been fixed at  $M_h = 90, 100, 110, 120$  and  $130 \text{ GeV}$ .

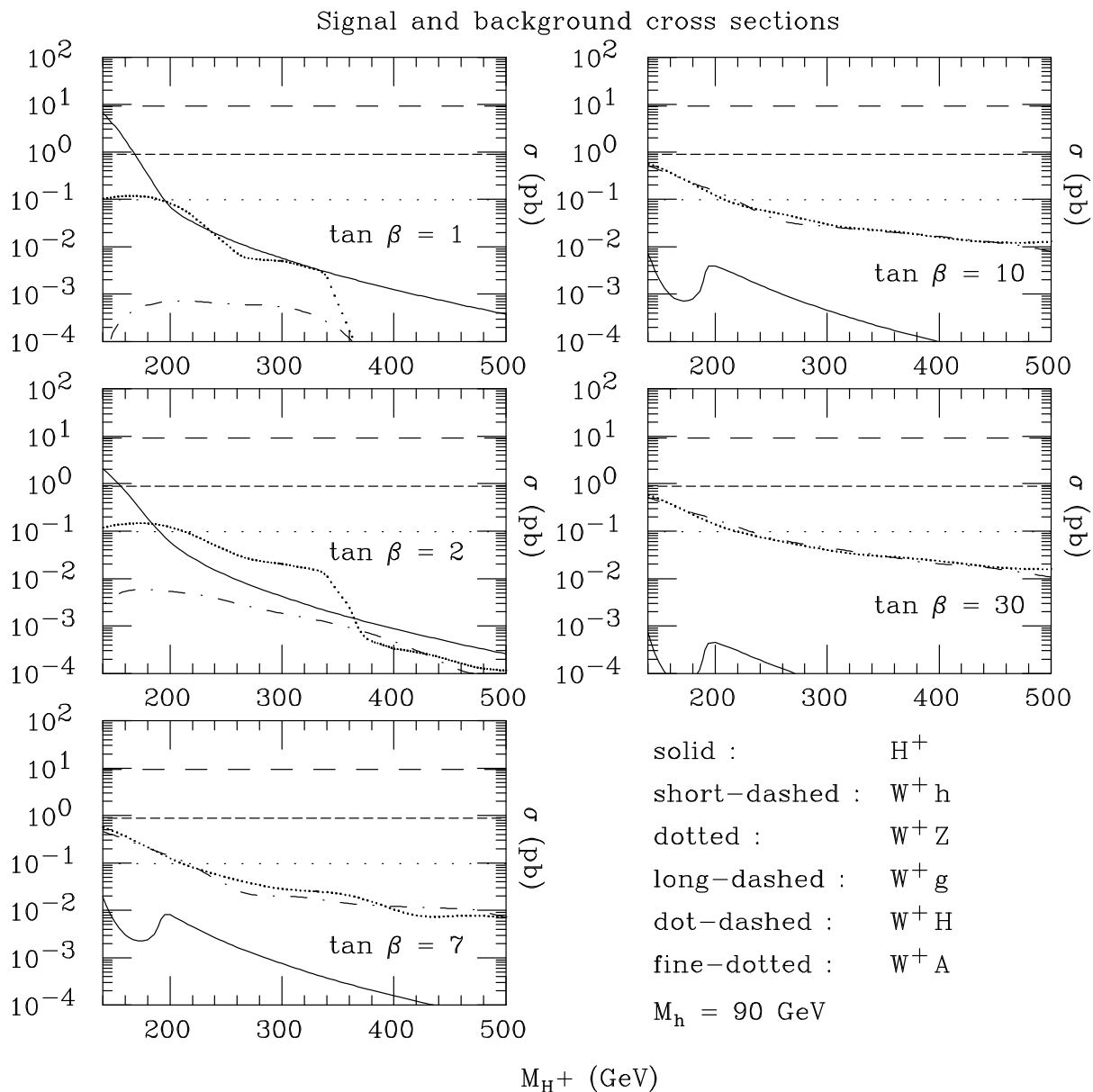


Figure 3: Cross sections of signal and backgrounds for selected values of  $\tan\beta$  over the mass range  $140\text{ GeV} \lesssim M_{H^\pm} \lesssim 500\text{ GeV}$ . The mass of the lightest Higgs boson has been fixed at  $M_h = 90\text{ GeV}$ . Here, both the top quark and the  $W^\pm$  boson are kept on-shell and no decay rates and cuts are applied.

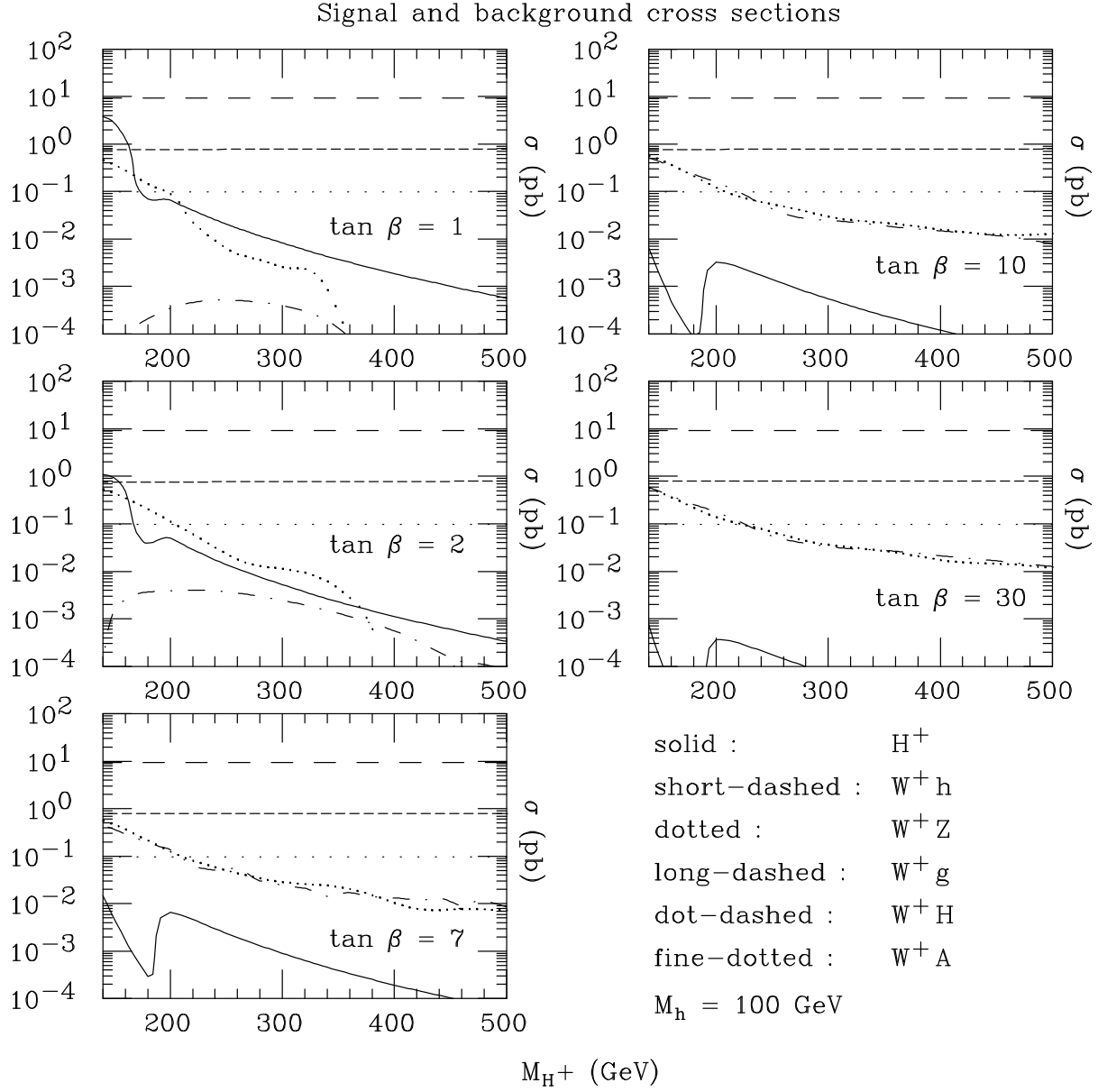


Figure 4: Same as Fig. 3 for  $M_h = 100 \text{ GeV}$ .

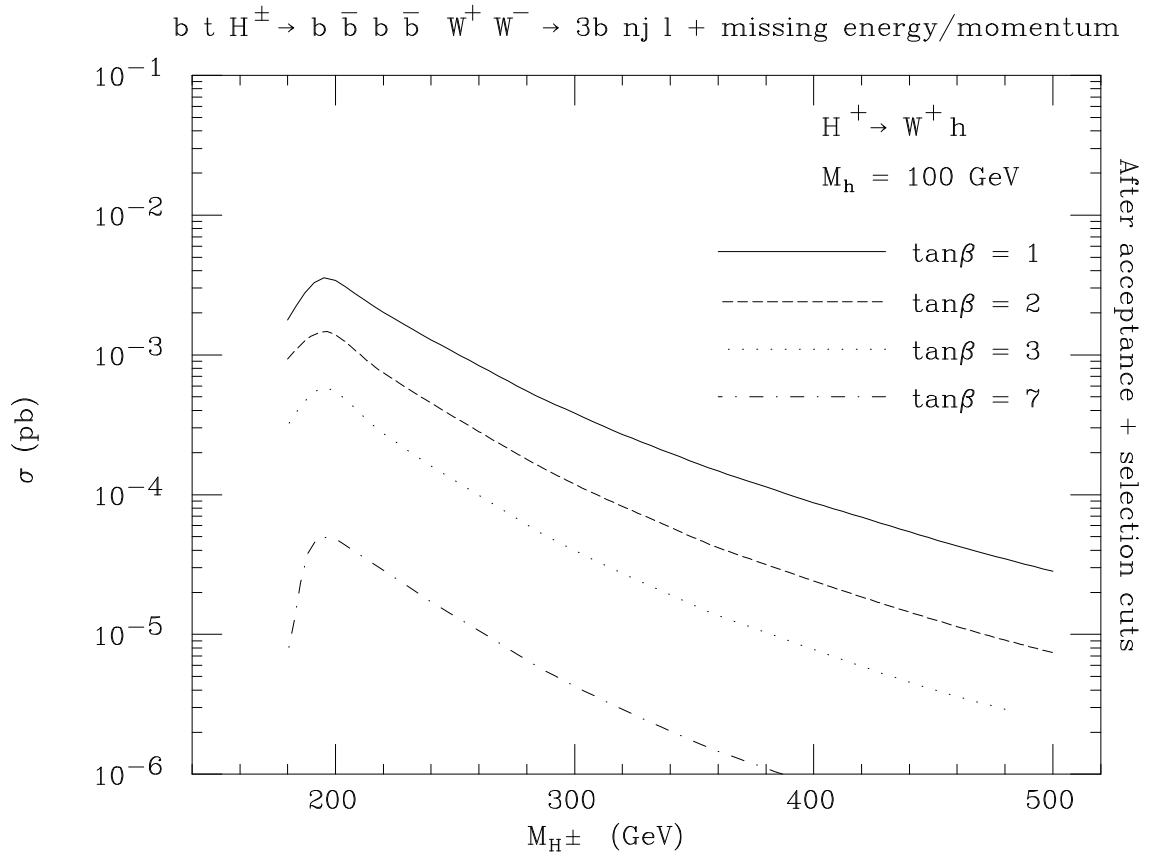


Figure 5: Cross sections of signal and backgrounds for selected values of  $\tan\beta$  over the mass range  $160 \text{ GeV} \lesssim M_{H^\pm} \lesssim 500 \text{ GeV}$ , after the cuts (3)–(9) and including decay rates. The mass of the lightest Higgs boson has been fixed at  $M_h = 100 \text{ GeV}$ .

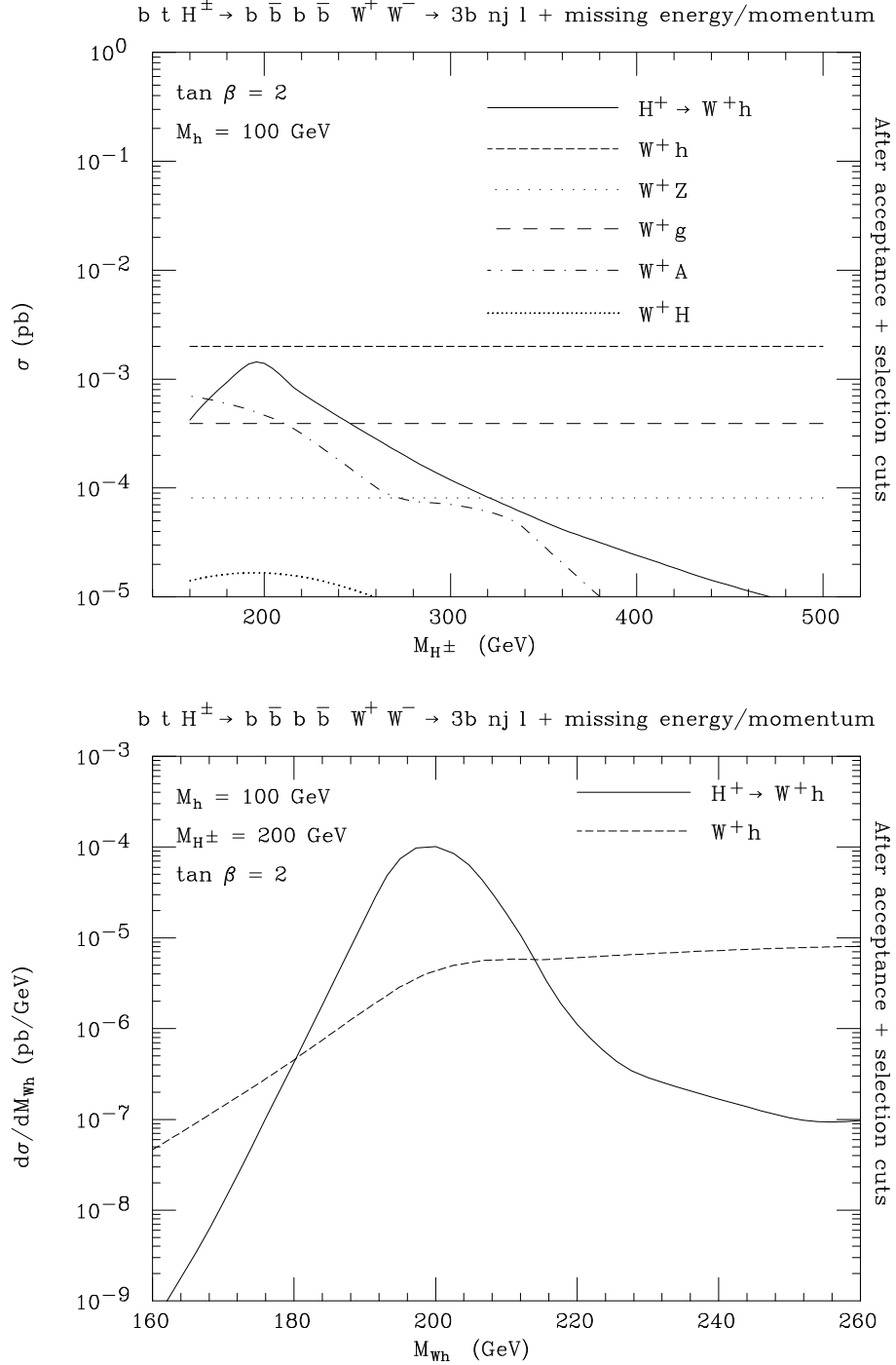


Figure 6: (Top) Total cross sections of signal and backgrounds for  $\tan \beta = 2$  and  $M_h = 100$  GeV after the cuts (3)–(9) and including decay rates, as a function of the charged Higgs boson mass over the range  $160 \text{ GeV} \lesssim M_{H^\pm} \lesssim 500 \text{ GeV}$ . (Bottom) Differential cross sections in the reconstructed  $W^\pm h$  invariant mass, for a  $M_{H^\pm} = 200$  GeV signal and for the dominant background after the cuts (3)–(9) and including decay rates. Gaussian smearing of all transverse momenta is included: with  $(\sigma(p_T)/p_T)^2 = (0.60/\sqrt{p_T})^2 + (0.04)^2$  for jets and  $(\sigma(p_T)/p_T)^2 = (0.12/\sqrt{p_T})^2 + (0.01)^2$  for leptons/missing particles.